CYCLONE STRUCTURAL TESTING STATION
JAMES COOK UNIVERSITY

INTERNAL AND NET PRESSURES ON LOW-RISE FULL-SCALE BUILDINGS

by

J. D. Ginger

TECHNICAL REPORT No 45

December 1997

CYCLONE STRUCTURAL TESTING STATION

INTERNAL AND NET PRESSURES ON LOW-RISE FULL-SCALE BUILDINGS

J. D. Ginger

Abstract

Full-scale measurements, theoretical analysis and numerical simulations were carried out to investigate internal pressures and net pressures on the WERFL test building at Texas Tech. The mean and fluctuating internal pressure coefficients were small in the nominally sealed building, and increase with increasing windward/leeward open area ratio. The effects of building flexibility on the internal pressure fluctuations were accounted for by increasing the volume of the building by a factor of K_A/K_B. Internal pressure fluctuations above a characteristic frequency were attenuated in the nominally sealed building which results in a small internal pressure gust factor. The internal pressure energy was increased close to the Helmholtz frequency in the building with a dominant opening. Wind load standards (ie. AS1170.2) generally provide conservative net pressure estimates for cladding design of a nominally sealed building, but underestimate the net cladding design pressure on small areas in regions near the roof windward edge of a building with a dominant windward wall opening.

INTERNAL AND NET PRESSURES ON LOW-RISE FULL-SCALE BUILDINGS

TABLE OF CONTENTS

1. INTRODUCTION

The approach wind and its flow around a building generates a spatially and temporally varying external pressure field on the building. The internal pressure then depends on this external pressure field, the position and size of all openings connecting the interior of the building to the exterior, the volume of the building and the flexibility of the envelope. The porosity ε, (defined as the ratio of effective leakage area to the surface area of the building) of a typical, nominally sealed building envelope ranges from 10^{-4} to 10^{-3}. The internal pressure in such a building is generally small in magnitude compared to external pressures. An opening created in the envelope by, say an open window or from debris impact etc., can generate large internal pressures in strong winds. The combination of large external and internal pressures acting in the same direction will create large net pressures across the envelope, and is a common cause of roof and wall failures in wind storms. This scenario often becomes the governing criterion for cladding and component design.

Following the initial work on internal pressure in low-rise buildings by Liu (1978), Holmes (1979), Stathopoulos et al (1979), Kramer et al (1979) and Liu and Saathoff (1981), more detailed studies have been carried out recently by Vickery (1986, 1991, 1994), Harris (1990) and Ginger et al (1995, 1997) Results from these theoretical, wind tunnel and full-scale studies form the basis of many of the latest wind load standards (ie. AS1170.2-1989, ASCE7-95).

External and internal pressures and their interaction were studied in detail at the Wind Engineering Research Field Laboratory (WERFL) low-rise full-scale building at Texas Tech University, for the cases of a nominally sealed building and building with large openings. The flexibility of the building and its effects on internal pressure fluctuations are accounted for by using the method of Vickery (1986). Comprehensive results from the full-scale WERFL study are presented in this paper. The internal pressure data are compared with analytical solutions and numerical simulations.

The WERFL test building and experimental set up are described briefly in Section 2. The theories on internal pressure and the effect of building flexibility are described in Section 3, and applied to the cases of a nominally sealed building and a building with large openings. The experimental results of this study are presented and compared with theoretical analysis, numerical simulations and with AS1170.2 in Section 4. The methods described by Vickery (1986) are used to estimate internal pressures in two example buildings in Section 5. The conclusions and recommendations are presented in Section 6.

2. THE TEST BUILDING AND FIELD MEASUREMENTS

The Wind Engineering Research Field Laboratory and instrumentation have been described by Levitan and Mehta (1992). The 9.1 (B) × 13.7 (D) × 4.0 (H) m rotatable WERFL test building is shown in Figure 1. The structural system consists of three H section steel frames spaced 7.0m and 5.5m apart in the 13.7m direction. Three C section columns are spaced equally apart on the 9.1 m walls. The roof span is 9.1m. Nine C section roof purlins span the 13.7m direction and are spaced symmetrically about the ridge at 1.5m, 3.1m, 3.8m and 4.6m from the ridge. Three C section wall girts run along all four walls of the building at elevations of 0.4, 1.2m and 2.6m. Load resisting cross braces are provided between the frames on the 13.7m walls and between the frames and the ridge for the roof. The building wall and roof envelope is of a sandwich construction, and consists of corrugated BRII steel inner cladding and flat stock exterior steel cladding with spacers in between.

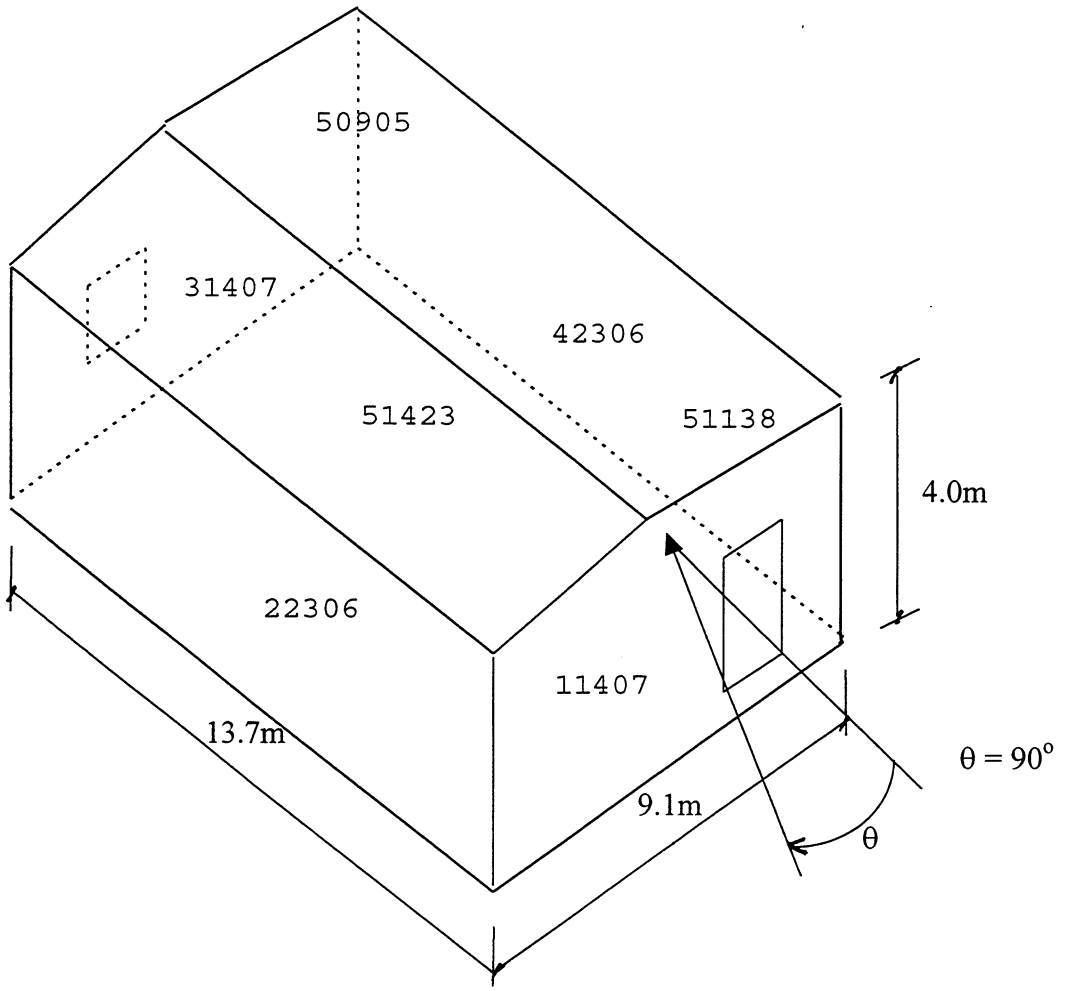

Figure 1. 13.7 × 9.1 × 4.0 m Wind Engineering Research Field Laboratory (WERFL) full scale low-rise test building at Texas Tech University Tap Locations •

The test building is equipped with instruments to record both internal and external pressures during strong winds. Wind speed and direction are measured at different heights on a meteorological tower located 46 m West of the building. The approach terrain is typically open (terrain category 2 as per AS1170.2), the topography flat and the turbulence intensity $\sigma_U / \overline{U}$, at roof height (ie. 4.0m) is ~ 0.20. The data acquisition and other electronic equipment are located in a 3.1 × 3.1 × 2.4 m enclosure, (containing an opening on the top), inside the building. The nominal internal volume of the test building including the instrument enclosure, V_I is estimated at 470 m^3.

Differential pressure transducers mounted adjacent to the surface pressure taps were used to measure external pressures (p_E) and the internal pressure (p_I). The pressure transducers were connected to the taps through flexible tubes, via electrical solenoid valves and have a good response to 20 Hz. The pressure signals were low-pass filtered at 8 Hz, and sampled at 30 Hz for a single run of 15 mins duration. The velocities were sampled at 10 Hz.

The mean, standard deviation, maximum and minimum pressure coefficients are defined as,

$$C_{\overline{p}} = \frac{\overline{p} - p_0}{\frac{1}{2}\rho\overline{U}^2}, \quad C_{\sigma p} = \frac{\sigma_p}{\frac{1}{2}\rho\overline{U}^2}, \quad C_{\hat{p}} = \frac{\hat{p} - p_0}{\frac{1}{2}\rho\overline{U}^2}, \quad C_{\breve{p}} = \frac{\breve{p} - p_0}{\frac{1}{2}\rho\overline{U}^2}$$

where,

$\bar{p},\sigma_p,\hat{p},\check{p}$	Mean, standard deviation, maximum and minimum pressure in a 15 min run
p_0	Reference pressure
ρ	Density of air
$\bar{U}$	Mean wind speed at roof height (ie. 4.0 m), over a 15 min run

The reference pressure (p_0) was obtained from a 1.4 × 1.1 × 1.0 m underground box with a 10mm diameter hole on the ground surface, located 23 m West of the building. The standard convention of defining positive and negative pressures acting towards and away from the surface respectively is used. The net (external-internal) pressures acting into and away from the building are defined positive and negative respectively. The results were obtained when $\bar{U}$ exceeds 8 m/s, and were from averaging up to six runs.

Data obtained for wind orientations (θ) of 90° ± 10°, and 270° ± 10° (ie. wind flow perpendicular to the 9.1m sides of building) are presented in this paper. External pressures were measured at tap locations 11407, 31407, 22306 and 42306 on the center of the windward, leeward and side walls, and 51423 and 50905/51138 on the center of the roof and roof windward edge (Levitan and Mehta (1992). The internal pressure was measured at different points within the building shown in Figure 1. Yeatts and Mehta (1993) found that the porosity, ε of the nominally sealed WERFL test building was in the range of 2×10^{-4} to 3×10^{-4} for an internal pressure range of 25 to 100 Pa. Windward wall openings (A_W) of 0.4, 0.8, 2.0 m^2 (ie. 1%, 2% and 5% of windward wall) and leeward wall openings (A_L) of 0.8, 2.0 m^2 (ie. 2% and 5% of leeward wall) were also tested for a range of A_W/A_L ratios in addition to the nominally sealed case.

3. THEORY

The unsteady discharge equation relating the flow (Q) through an opening of area A and the pressure drop (Δp) across the opening may be given by Equation 1.

$$\Delta p = \frac{1}{2} C_L \rho U_O^2 + C_I \rho \frac{\partial U_O}{\partial t} \sqrt{A} \qquad (1)$$

Here $U_O = (Q/A)$ is the area averaged velocity through the opening. The first term on the right hand side of Equation 1 represents the pressure drop due to viscous effects while the second is that required to accelerate the flow through the opening. The loss coefficient C_L is equivalent to $1/k^2$, where k was the discharge coefficient defined by Holmes (1979). The effective length of the slug of air accelerated through the opening, $l_e = C_I\sqrt{A}$. Vickery (1994) indicated that C_L and C_I can only be defined for limited situations such as a sharp edged circular opening connecting two large volumes, where potential flow theory gives $C_L = \left[(\pi+2)/\pi\right]^2 = 2.68$ and $C_I = \sqrt{\pi/4} = 0.89$. The applicability of these values in flows such as that of unsteady wind flow through openings in a building is however unclear.

3.1 Mean Internal Pressure

The principles of conservation of mass and steady flow through an opening are used to obtain the relationship between mean internal pressure ($\bar{p}_I$), mean external windward pressure ($\bar{p}_W$) and mean external leeward pressure ($\bar{p}_L$) in a building with total windward opening area A_W and total leeward opening area A_L as shown by Equation 2. This relationship is also used in AS1170.2 to derive the internal pressure coefficient for a given A_W/A_L ratio.

$$C_{\bar{p}_I} = \frac{C_{\bar{p}_W}}{1+\left(\frac{A_L}{A_W}\right)^2} + \frac{C_{\bar{p}_L}}{1+\left(\frac{A_W}{A_L}\right)^2} \qquad (2)$$

3.2 Internal Pressure Fluctuations

In addition to the external pressure field around the building and the position and size of all openings connecting the interior to the exterior, the response of internal pressure to external pressure fluctuations also depends on the volume of the building and the flexibility of the envelope.

There can be strong dynamic interaction between the building and the internal pressure in flexible structures. According to Vickery (1986) the degree of interaction depends on the following two factors.

(i) Natural frequency of vibration of the building envelope and frequency of pressure fluctuations.

The frequency of a low-rise building in the volume changing mode is mainly determined by the natural frequency of the roof system. Except for roofs with very large spans (> 20 m), this frequency will be greater than 1 Hz, and beyond the frequencies in the approach flow velocity. In addition, the pressure fluctuations are attenuated inside a nominally sealed building, compared with the external pressures, and the building response may be considered to follow the wind loads in a quasi-static manner. However, for some buildings containing a dominant opening, there is a possibility that the Helmholtz frequency (as described in section 3.2.2), may fall close to the natural frequency of the roof system resulting in increased dynamic interaction between the internal pressure and the building. If the frequency of internal pressure fluctuations is comparable with the frequency of the building envelope the situation is highly complex as described by Vickery and Georgiou (1991) and is beyond the scope of this paper.

(ii) Ratio of bulk modulus of the building (defined as the internal pressure change required for a unit volumetric strain), to the bulk modulus of the air contained in the building.

When a building is flexible, the internal volume V_I, will expand and contract with the changes in internal pressure. The internal pressure response is slowed as this additional change in volume must also pass through the openings. Vickery (1986) showed that this effect can be incorporated into the analysis by determining the volumetric change of the building due to an increase in internal pressure and the magnitude of this compared to the volumetric change of the air contained within the building. The internal pressure dynamics in both nominally sealed buildings and buildings with a dominant opening may be analyzed by replacing the nominal internal volume V_I by an effective

internal volume, $V_{Ie} = V_I\left(1+\frac{K_A}{K_B}\right)$, where K_A/K_B is the ratio of bulk modulus of the air contained in the building to the bulk modulus of the building (ie. internal pressure change for unit volumetric strain, $\Delta p_I/(\Delta V_I/V_I)$).

The bulk modulus of the WERFL test building, K_B was determined by pressurizing the nominally sealed building and measuring the deflections at several points on the wall and roof. The bulk modulus of air $K_A = n \times p_0$, where n = 1.4 for an adiabatic process. This data was used to estimate K_A/K_B at 1.5. The effects of WERFL building flexibility on internal pressure fluctuations in the nominally sealed and building with openings are therefore accounted for by using an effective internal volume $V_{Ie} = V_I \times (1 + K_A/K_B) = 470 \times (1 + 1.5) = 1175\ m^3$.

3.2.1 Nominally Sealed Building

Vickery (1986) and Harris (1990) studied the internal pressure fluctuations in a nominally sealed building where the openings on the envelope are small and uniformly distributed. The inertia term in Equation 1 is discarded, and opening areas A_W on the surfaces having higher pressures than the interior and opening areas A_L on the surfaces having lower pressures than the interior are combined such that $\Delta C_{\bar{p}} = C_{\bar{p}_W} - C_{\bar{p}_L}$ is the net mean pressure difference between these *"windward"* and *"leeward"* surfaces. The internal pressure response to changes in external pressure may be described by a characteristic response time T_C and a characteristic frequency f_C;

$$f_C = \frac{1}{2\pi}\left(\frac{1}{T_C}\right) = \frac{1}{2\pi}\left(\frac{a_s^2(A_W^2 + A_L^2)^{3/2}}{V_{Ie}\bar{U}A_W A_L(C_L\Delta C_{\bar{p}})^{1/2}}\right) \qquad (3)$$

where $a_s = (K_A/\rho)^{1/2}$ is the speed of sound $\quad K_A = n \times p_0 \quad$ n = 1.4 for an adiabatic process.

The interpretation of in Equation 3, by Vickery (1986) was that external pressure fluctuations above the frequency f_C, (time scales smaller than T_C) are attenuated and not passed effectively into the building. T_C is the appropriate averaging time for determining peak internal pressures.

3.2.2 Building Containing a Dominant Opening

A dominant opening may be defined albeit imprecisely as an opening *"large enough"* to have a significant impact on the internal pressure, such as an opening of area greater than about twice the total background leakage area. In such a case the appropriate approach is to examine the equations of motion of air in a sealed building with a single dominant opening. However, Vickery and Bloxham (1992) found that the magnitude of internal pressure fluctuations was progressively reduced as the total background leakage area was increased beyond 10% of the dominant opening.

Holmes (1979) and Vickery (1986) derived Equation 4 to study the time dependent motion of air in a building with a dominant opening of area A, in terms of internal pressure coefficient C_{p_I} and external pressure coefficient at the opening, C_{p_E}.

$$\frac{C_I V_{Ie}}{a_s^2\sqrt{A}}\ddot{C}_{PI} + C_L\left[\frac{V_{Ie}\overline{U}}{2Aa_s^2}\right]^2 \dot{C}_{PI}\left|\dot{C}_{PI}\right| + C_{p_I} = C_{p_E} \tag{4}$$

Equation 4 is a second order differential equation of a single degree of freedom dynamic system with non-linear (square law) damping. The first term in Equation 4, represents the inertia of the slug of air moving in and out of the opening. The second damping term represents the energy lost in the process and the third stiffness term represents the resistance to deflection of the air in the building. The term on the right hand side in Equation 4 is the change in external pressure which forces the air in and out of the opening.

Holmes (1979) and Liu and Rhee (1986) carried out wind tunnel model studies for a range of dominant windward and leeward opening areas and showed that internal pressure resonance occurs close to the undamped Helmholtz frequency, $f_0 = \frac{1}{2\pi}\left(\frac{a_s^2\sqrt{A}}{C_I V_{Ie}}\right)^{1/2}$. They also showed that there was an increasing tendency for resonance to occur as the opening area increases relative to the internal volume. Equation 4 shows that damping is reduced as the ratio of opening area to internal volume is increased. It should however be noted that the porous envelope of most buildings helps attenuate the Helmholtz resonance to some degree.

It is also of interest to compare the internal pressure energy with the external pressure energy at the opening, for a building containing a dominant opening. Vickery and Bloxham (1992) derived a relationship between the fluctuating internal pressure and external pressure at the opening in terms of the standard deviation of the external and internal pressures in Equation 5. The ratio of internal to external pressure standard deviation may be used to gauge the effect of Helmholtz resonance.

$$C_{\sigma pI}/C_{\sigma pE} = \left[(1-1.5S_o) + \left[\pi^3 S_o^2/\left(32\beta^4 C_{\sigma pE}^2\right)\right]^{1/3}\right]^{1/2} \tag{5}$$

where $S_o = f_o S_{pE}(f_o)/C_{\sigma pE}^2$, (6)

where S_{pE} Power Spectral Density of External Pressure and

$$\beta = \frac{1}{2}\left(\frac{C_L}{C_I}\right)^{1/2}\frac{\overline{U}}{a_s}\sqrt{V_{Ie}}A^{-3/4} \tag{7}$$

3.3 Quasi-Steady Theory and Gust Factors

Many wind load standards (ie. AS-1170.2, ASCE7-95) use the quasi-steady approach for obtaining design wind loads on low-rise buildings. As described in Equation 8 by Holmes (1981), a mean pressure coefficient $C_{\bar{p}}$ is multiplied by the design 3 sec gust pressure in this method to obtain peak external and internal pressures. A local pressure factor such as K_L in AS1170.2 is provided to account for the larger pressures near edge discontinuities (ie. ridge line etc.). AS1170.2 prescribes a local pressure factor K_L of 1.5 and 2.0 to be applied with negative pressures on areas of extent less than $1.0a^2$ and $0.25a^2$ within a distance of 1.0a and 0.5a respectively from edge discontoinuities, where the dimension 'a' is taken to be the minimum of 0.2B or 0.2D or H. The appropriate local pressure factor K_L was included in the analysis, with a = 1.8m. The net wind loads on cladding and

structural components are then determined by combining these peak external and internal pressures acting in the same direction. This implies that the pressure fluctuations follow the approach flow velocity fluctuations and the ratio of design peak pressure p_{pk} to mean pressure $\bar{p}$ is related to the velocity gust factor $G_U = \hat{U}_{3s}/\overline{U}$ by Equation 9.

$$p_{pk} = \left(\tfrac{1}{2}\rho \hat{U}_{3s}\right)C_{\bar{p}} \tag{8}$$

$$C_{pk} / C_{\bar{p}} = \left(\hat{U}_{3s}/\overline{U}\right)^2 = G_U^2 \tag{9}$$

Greenway (1979) obtained an analytical expression for wind velocity gust factor $G_U = \hat{U}/\overline{U}$ from which the mean velocity is scaled up to obtain a maximum gust wind speed $\left(\hat{U}\right)$ in that period. The analysis is based on the assumptions that the longitudinal velocity spectrum is of the von Karman form and the probability distribution of the wind velocity being of the Gaussian form. Following on Vickery (1986) showed that the internal pressure gust factor G_{pI} can be expressed by Equation 10.

$$G_{pI} = 1 + 2g_U \frac{\sigma_u(f_C)}{\overline{U}} \tag{10}$$

$$\text{where } \sigma_U^2(f_C) = \int S_U(f) / (1 + {}^{f}\!/_{f_C})^2 df \tag{11}$$

Here $S_U(f)$ is the power spectral density of the longitudinal velocity.

$$\text{and } g_U = \sqrt{2\ln\nu T} + 0.58/\sqrt{2\ln\nu T} \tag{12}$$

$$\nu^2 = \int f^2 S_U(f) / (1 + {}^{f}\!/_{f_C})^2 df \tag{13}$$

Vickery (1986) suggests using $T_C = 1/f_C$ as the appropriate averaging time for determining the peak value. The internal pressure gust factor G_{pI} is dependent on the turbulence intensity and the frequency parameter ${}^{f_C L_U}\!/_{\overline{U}}$, where L_U is the integral length scale of turbulence. Vickery (1986) presented Figure 2, which can be used to determine the values of ${}^{\sigma_U(f_C)}\!/_{\sigma_U}$ and ${}^{\upsilon L_U}\!/_{\overline{U}}$ as a function of ${}^{f_C L_U}\!/_{\overline{U}}$ for a spectrum of the form $\dfrac{fS_U(f)}{\sigma_U^2} = {}^{4\left(fL_U/\overline{U}\right)}\!/_{\left[1 + 70.8\left(fL_U/\overline{U}\right)\right]^{5/6}}$.

4. RESULTS

The results of this study are presented in two separate parts; the nominally sealed building and the building containing large openings. The external and internal pressure data collected are analyzed and compared with theoretical and numerical simulations and values derived from AS1170.2.

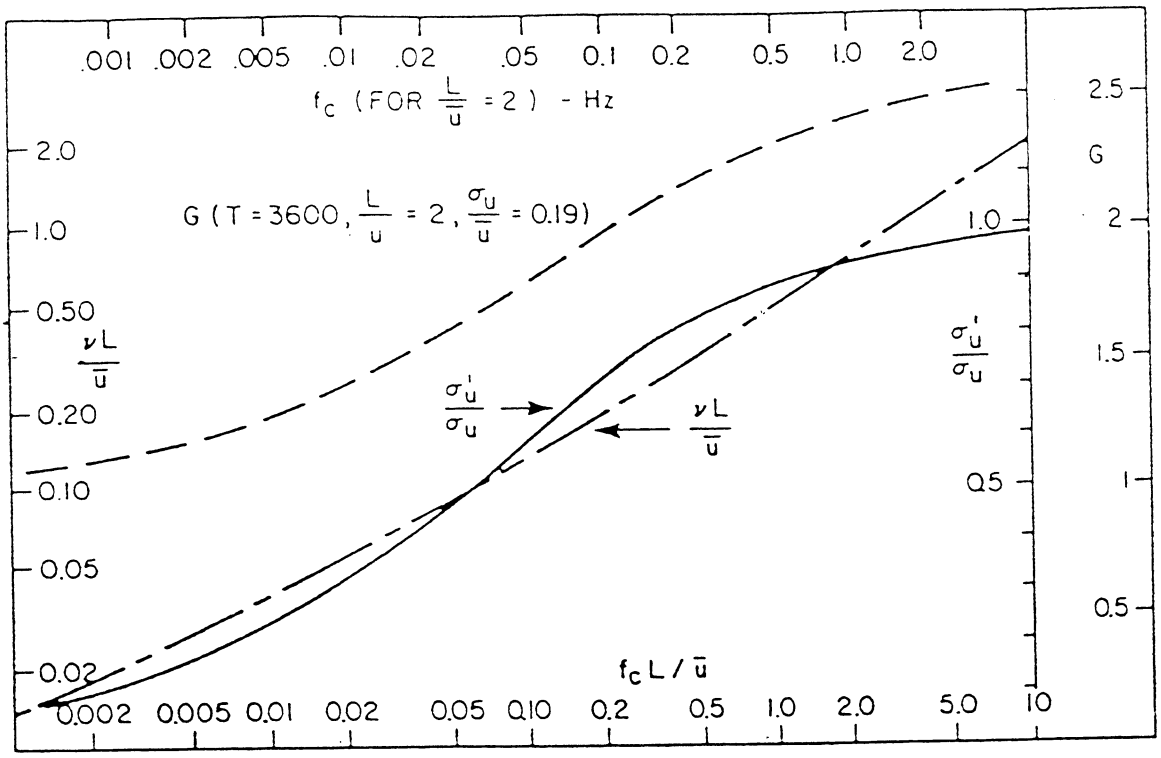

Figure 2. Gust Factor Parameters (From Vickery (1986))

The longitudinal velocity spectrum of the approach flow at roof height (ie. 4.0 m), $fS_U(f)/\sigma_U{}^2$ and the pressure spectra $fS_p(f)/\sigma_{pW}{}^2$ on the windward wall and roof windward edge are shown in Figure 3. The velocity and pressure spectra are non-dimensionalised by the variance of the velocity at roof height and the variance of the windward wall pressure respectively. Although the pressure measurement system has a good response up to 8 Hz, the velocity measurement system can only respond up to about 0.2 Hz, beyond which the velocity signal is attenuated. Therefore comparisons of these spectra beyond 0.2 Hz are not possible. Figure 3 shows that the windward wall pressure spectrum closely follows the approach flow velocity spectrum up to ~ 0.2 Hz, and the quasi-steady method may be satisfactorily used for determining the design wind loads on the windward wall center as suggested by Kawai (1983). The roof windward edge pressure spectrum contains more energy over the entire range of frequencies compared with the windward wall pressure spectrum.

The non-dimensional pressure spectra $fS_p(f)/\left(\frac{1}{2}\rho\bar{U}^2\right)^2$ on the windward wall, leeward wall, side wall and roof center and roof windward edge are shown in Figure 4. This shows that the side wall, roof center and leeward wall pressure spectra contain progressively less energy compared with the windward wall pressure. The pressure fluctuations on the leeward wall, side wall and roof are influenced by flow separation as indicated by the distribution of energy in Figure 3 and Figure 4. This is in agreement with Kawai's (1983) analysis which showed that the quasi-steady method is not applicable in these areas which are influenced by the building or affected by flow separation.

$$\frac{fS_U(f)}{\sigma_U^2}$$

$$\frac{fS_p(f)}{\sigma_{p_W}^2}$$

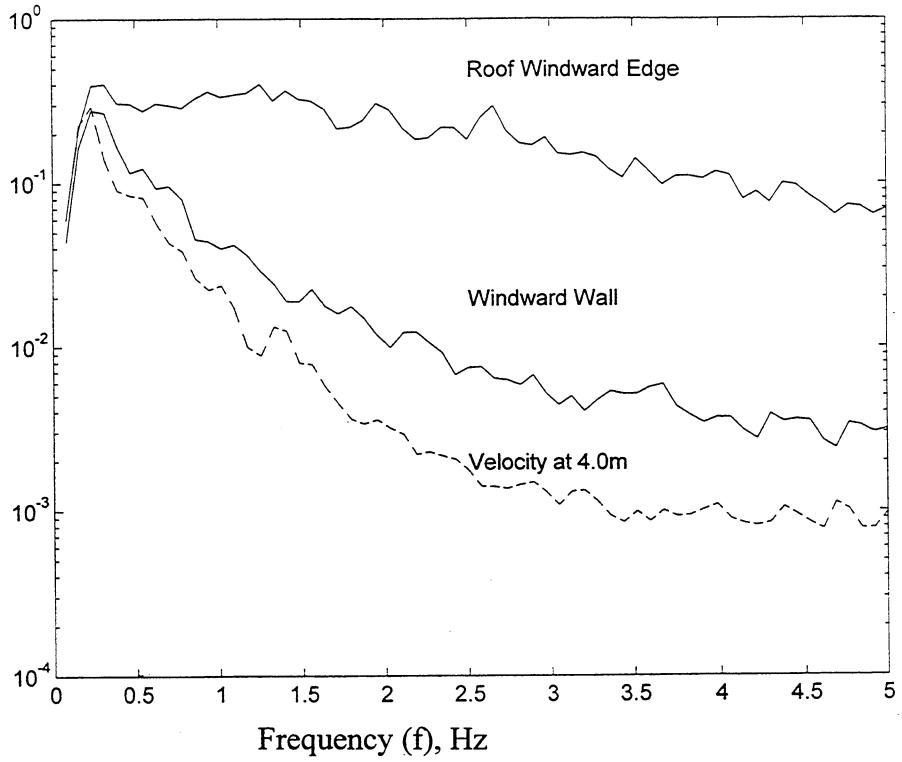

Figure 3. Non-dimensional, Velocity Spectrum at Roof Height (ie. 4.0m) and Windward Wall and Roof Windward Edge Pressure Spectra

$$\frac{fS_p(f)}{\left(\frac{1}{2}\rho\bar{U}^2\right)^2}$$

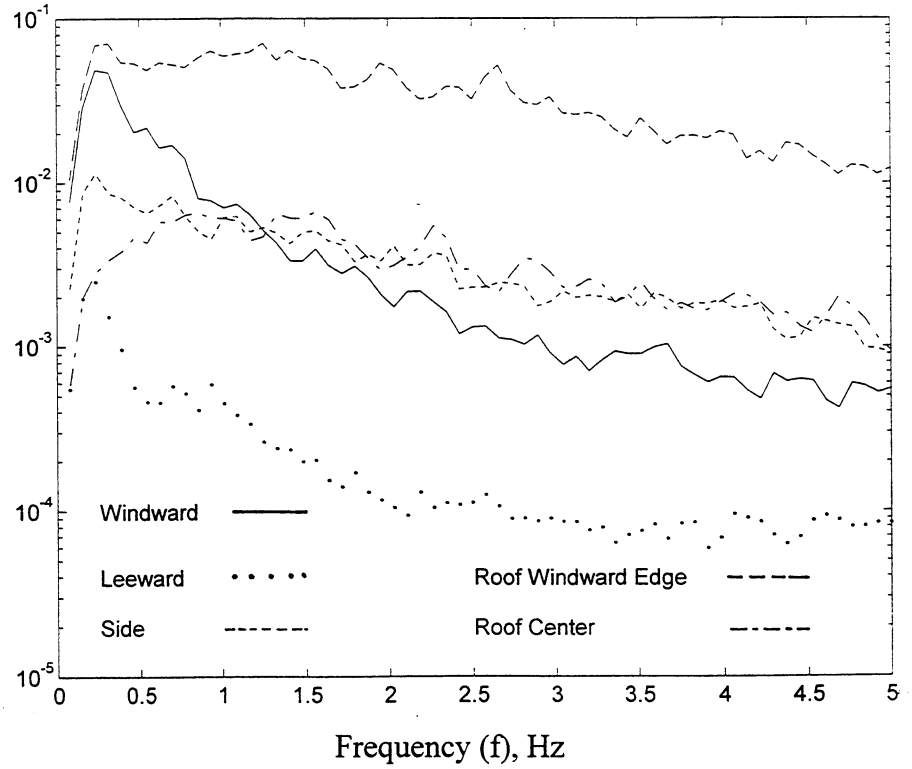

Figure 4. Non-dimensional Pressure Spectra on Windward Wall, Leeward Wall, Side Wall, Roof Windward Edge and Roof Center

4.1. Nominally Sealed Building

A part of the measured windward wall pressure, roof windward edge pressure and internal pressure on the nominally sealed WERFL test building is shown in Figure 5a. The resultant net pressures on the windward wall and roof windward edge are shown in Figure 5b. The internal pressure fluctuations are small compared with the external pressure fluctuations. Yin (1994) found that the internal pressure in the nominally sealed WERFL test building was uncorrelated with external pressures.

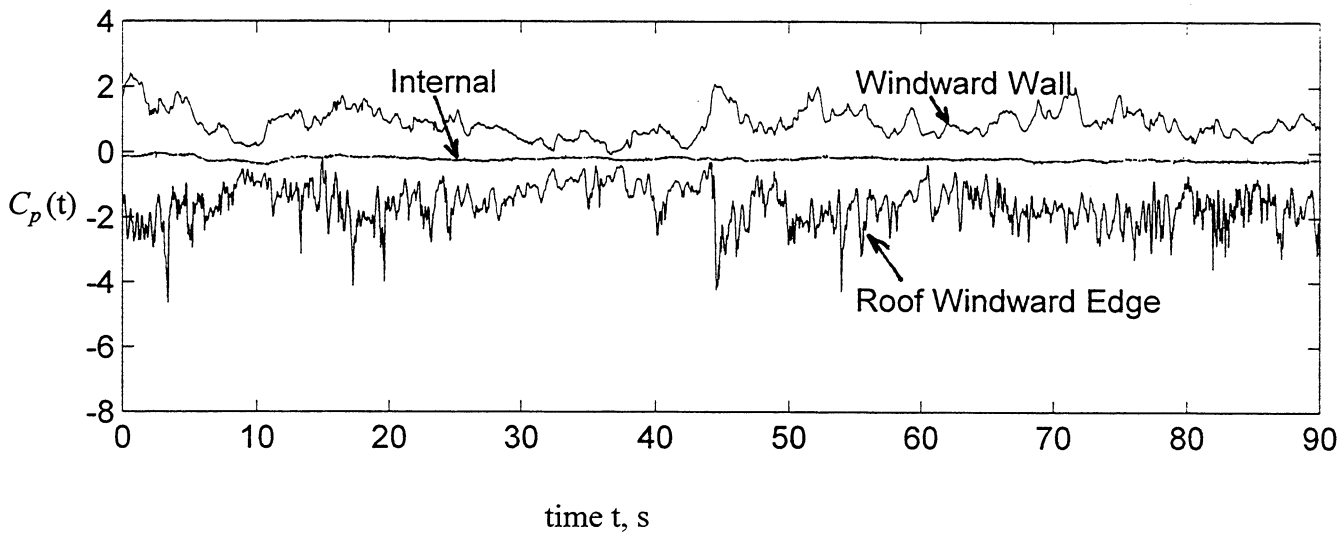

Figure 5a. Windward Wall, Windward Roof Edge and Internal Pressure Coefficient vs Time - Nominally Sealed Building

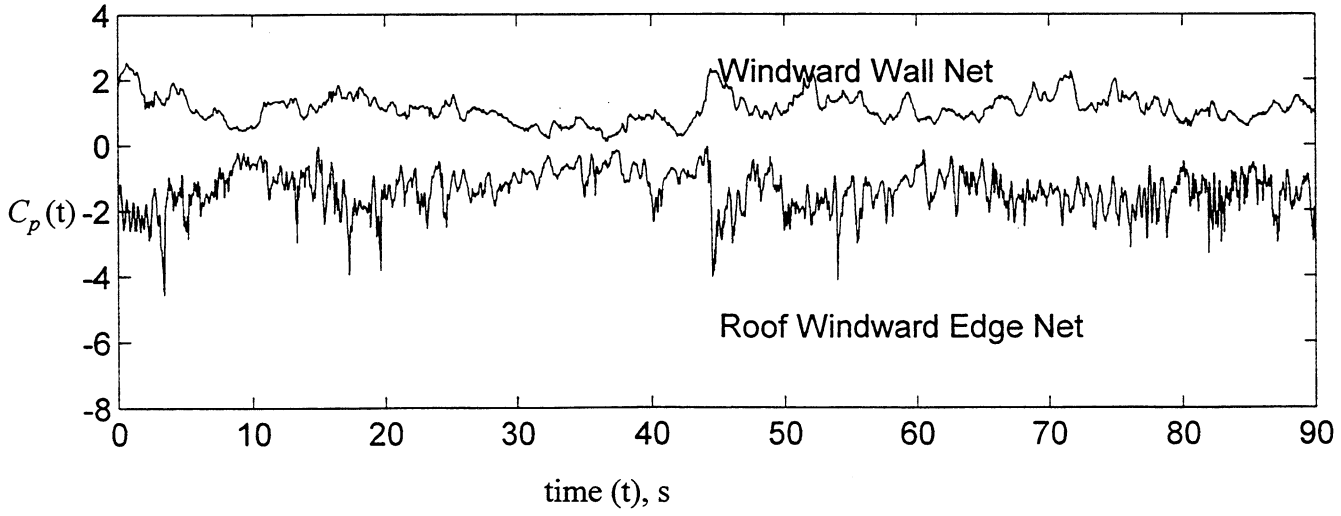

Figure 5b. Windward Wall and Windward Roof Edge Net Pressure Coefficient vs Time - Nominally Sealed Building

The mean, standard deviation, maximum and minimum pressure coefficients and the pressure peak factors, $g_p = |p_{pk} - \bar{p}|/\sigma_p$ and pressure gust factors, $G_p = p_{pk}/\bar{p}$ on the windward wall, leeward wall, side wall, roof, roof windward edge and interior of the nominally sealed WERFL test building, and the pressure coefficients from AS1170.2 (K_L = 1.5 is applied to the roof windward edge for pressure acting on an area ~ 0.5 m^2, 1.5 m from the edge) are given in Table 1a.

Table 1a. External and Internal Mean, Standard Deviation, Maximum and Minimum Pressure Coefficients - Nominally Sealed Building

Tap Location	Pressure Coefficients					g_p	G_p
	AS1170	$C_{\bar{p}}$	C_{σ_p}	$C_{\hat{p}}$	$C_{\check{p}}$		
Windward Wall Center	0.7	0.70	0.39	2.76	-0.22	5.28	3.94
Leeward Wall Center	-0.4	-0.34	0.12	0.00	-0.85	4.25	2.50
Side Wall Center	-0.5	-0.29	0.24	0.52	-1.95	6.92	6.72
Roof Center	-0.5	-0.27	0.18	0.66	-1.72	8.06	6.37
Roof Windward Edge	-1.35	-1.04	0.42	0.01	-3.52	5.90	3.38
Internal	0, -0.3	-0.14	0.06	0.09	-0.38	4.00	2.71

The windward wall experiences a mean positive pressure and the leeward wall, side walls and roof experience mean suction pressures. The mean internal pressure is small and negative. The pressure gust factor G_p is the ratio between the peak pressure and mean pressure averaged over 15 min, and depends on the mean value and the characteristics of the fluctuations. The windward wall pressure fluctuations are generated by the approach flow velocity fluctuations and the pressure gust factor $G_{p_W} = \hat{p}_W/\bar{p}_W$ = 2.76/0.70 = 3.94. Flow separation, re-attachment and roll-up generates large intermittent suction pressures at the center of the roof and side walls and this results in larger pressure gust factors while the small pressure fluctuations in the wake behind the leeward wall results in a smaller pressure gust factor. The pressure fluctuations are damped inside the nominally sealed building which results in a small internal pressure gust factor $G_{pI} = \check{p}_I/\bar{p}_I$ = -0.38/-0.14 = 2.71. The external pressure peak factor values range from 4.25 to 8.06 and the internal pressure peak factor was 4.00.

The peak net (external - internal) pressure coefficients are compared with the (peak external - peak internal) pressure coefficients shown within parenthesis and the equivalent net values derived from AS1170.2 in Table 1b. A velocity gust factor G_U = 1.75 for 4.0 m in terrain category 2 (AS1170.2) is applied to Equation 9, and the worst combinations of C_{pI} and C_{PE} are used to calculate the equivalent AS1170.2 net C_{pk} values.

The measured peak net pressures shown in Table 1b are 76% to 90% in magnitude of the (peak external - peak internal) pressures. AS1170.2 provides conservative peak net pressures on the center of the windward wall, roof windward edge, center of the leeward wall, center of the side walls and the center of the roof.

Table 1b. Net, Mean, Standard Deviation, Maximum and Minimum Pressure Coefficients - Nominally Sealed Building

Tap Locations	Net Pressure Coefficients					
	AS1170.2		Measured			
	$C_{\bar{p}}$	C_{pk}	$C_{\bar{p}}$	C_{σ_p}	$C_{\hat{p}}$	$C_{\check{p}}$
Windward Wall Center	1.0	3.06	0.84	0.43	2.83 (3.14)	-0.09 (-0.31)
Leeward Wall Center	-0.4	-1.23	-0.20	0.09	0.22 (0.38)	-0.73 (-0.94)
Side Wall Center	-0.5	-1.53	-0.15	0.23	0.50 (0.90)	-1.55 (-2.04)
Roof Center	-0.5	-1.53	-0.13	0.18	0.65 (1.04)	-1.38 (-1.81)
Roof Windward Edge	-1.35	-4.13	-0.90	0.39	0.06 (0.39)	-3.22 (-3.61)

A smoke exfiltration study was carried out in the nominally sealed WERFL test building which indicated that leakage took place around the door and window clearances, and at the joints and connections on the walls and roof. Assuming the porosity is uniform over the whole WERFL test building envelope, for an approach wind flow normal to the 9.1 m side of the building, the ratio of leakage areas on the windward wall, leeward wall, two side walls and roof is 1 : 1 : 3 : 3.5. Using mean pressure coefficients of +0.70 on the windward wall, -0.34 on the leeward wall, -0.29 on the side walls and -0.27 on the roof, and the "windward" to "leeward" leakage ratio A_W/A_L = 1/7.5, $C_{\bar{p}_W}$ = 0.70, $C_{\bar{p}_L}$ = -0.29 and $\Delta C_{\bar{p}}$ = 0.99.

For the WERFL test building of height H = 4.0 m and breadth B = 9.1 m normal to the wind, Equation 3 may be reduced to Equation 14, where r = A_W/ A_L.

$$f_C = \frac{1}{2\pi}\left(\frac{\varepsilon H B a_s^2 r^{-1/2}(r+r^{-1})^{3/2}}{V_{Ie}\bar{U}\sqrt{C_L}\sqrt{\Delta C_{\bar{p}}}}\right) \tag{14}$$

The characteristic frequency f_C for the nominally sealed WERFL building with uniform porosity ε, = 2.5 × 10^{-4}, r = 1/7.5 and V_{Ie} = 1175 m^3, determined from Equation 14, is 0.5 Hz, by applying typical values of mean wind speed at roof height $\bar{U}$ = 10 m/s, a_s = 333 m/s, $\Delta C_{\bar{p}}$ =0.99 and C_L = 2.68.

The longitudinal length scale L_U at roof height (ie. 4.0m) at the WERFL site was estimated at about 120m by Thomas et. al. (1993). For f_C = 0.5 Hz and $\bar{U}$ = 10 m/s, $f_C L_U/\bar{U}$ = 6.0. Using Figure 2 from Vickery (1986), $\upsilon L_U/\bar{U}$ = 1.2, υ = 0.1 and $\sigma_U(f_C)/\sigma_U$ = 0.98. For T = 15 min = 900s, υT=90, and from Equation 12, g_u = 3.19, $\sigma_U(f_C)/\bar{U}$ = 0.98 × 0.23 = 0.225 and from Equation 10, G_{pI} = 2.44 which is 90% of the 2.71 obtained experimentally and given in Table 1a.

The pressure spectra $fS_p(f)/\left(\frac{1}{2}\rho\bar{U}^2\right)^2$ for windward wall, roof windward edge and interior of the nominally sealed building are presented in Figure 6. The internal pressure fluctuations contain much less energy compared with the external pressure fluctuations, and are significantly attenuated above 0.4 Hz with a sharp drop off, in agreement with the theoretical analysis (ie. Equation 14).

The net (external - internal) pressure spectra $fS_p(f)/\left(\frac{1}{2}\rho\bar{U}^2\right)^2$ on the windward wall, and roof windward edge of the nominally sealed building are shown in Figure 7. The net pressure spectra on each part of the WERFL building has a similar form to the external pressure spectra in Figure 6.

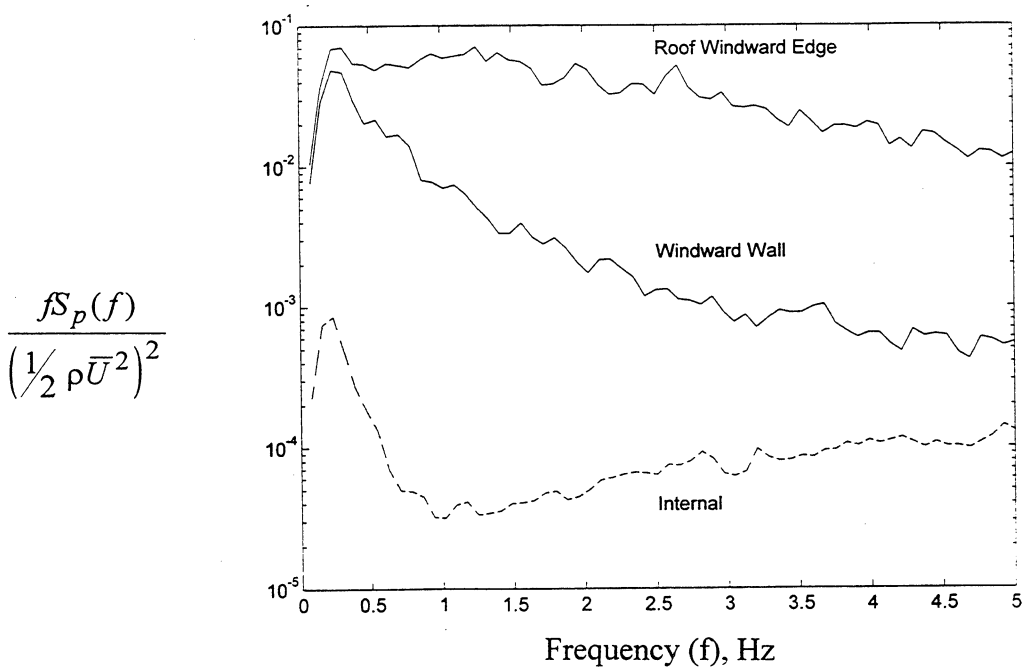

Figure 6. Non-dimensional Windward Wall, Roof Windward Edge and Internal Pressure Spectra - Nominally Sealed Building

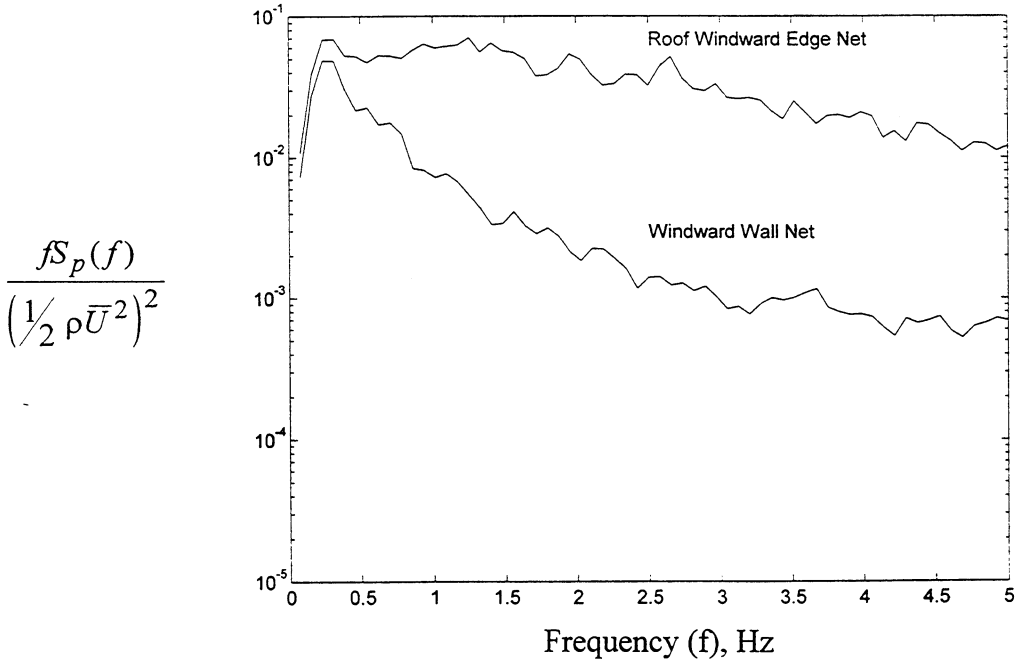

Figure 7. Non-dimensional Windward Wall and Roof Windward Edge Net Pressure Spectra - Nominally Sealed Building

4.2 Building Containing Large Opening(s)

The mean, standard deviation, maximum and minimum pressure coefficients obtained on the windward wall, leeward wall and interior, for a range of windward and leeward wall opening A_W/A_L ratios of WERFL test building (background porosity neglected) are given in Table 2. For a single wall opening, the internal pressure closely follows the pressure on the wall containing the opening. In a building with windward and leeward wall openings, the mean and fluctuating internal pressures are influenced by the pressures on both the windward and leeward walls. Figure 8 shows the variation of the mean, standard deviation, maximum and minimum internal pressure coefficients with A_W/A_L ratio and the mean internal pressure plot from Equation 2 for $C_{\bar{p}_W} = 0.65$ and $C_{\bar{p}_L} = -0.30$. The experimental mean internal pressure data agrees with the theoretical analysis of flow through an orifice as did the results of Holmes (1979).

Table 2. Mean, Standard Deviation, Maximum and Minimum Windward Wall, Leeward Wall, and Internal Pressure Coefficients for the WERFL Test Building with Windward and/or Leeward Opening(s) (Background Porosity Neglected).

Openings		Pressure Coefficients											
A_W	A_L	Windward Wall				Leeward Wall				Internal			
(m^2)	(m^2)	$C_{\bar{p}}$	C_{σ_p}	$C_{\hat{p}}$	$C_{\check{p}}$	$C_{\bar{p}}$	C_{σ_p}	$C_{\hat{p}}$	$C_{\check{p}}$	$C_{\bar{p}}$	C_{σ_p}	$C_{\hat{p}}$	$C_{\check{p}}$
0.4	0.0	0.63	0.32	2.35	-0.15	-0.32	0.09	-0.05	-0.71	0.60	0.30	2.25	-0.18
0.8	0.0	0.62	0.42	2.76	-0.43	-0.43	0.13	-0.09	-0.95	0.61	0.42	2.74	-0.38
2.0	0.0	0.60	0.31	2.28	-0.16	-0.25	0.10	0.08	-0.61	0.60	0.31	2.20	-0.17
2.0	0.8	0.57	0.27	1.87	-0.11	-0.24	0.10	0.10	-0.46	0.46	0.24	1.90	-0.14
0.4	2.0	0.66	0.37	2.41	-0.28	-0.32	0.18	0.21	-0.90	-0.22	0.10	0.15	-0.64
0.8	2.0	0.65	0.36	2.29	-0.22	-0.28	0.16	0.16	-0.76	-0.13	0.10	0.36	-0.53
0.0	2.0	0.59	0.30	2.14	-0.20	-0.35	0.11	0.02	-0.78	-0.35	0.10	-0.02	-0.82

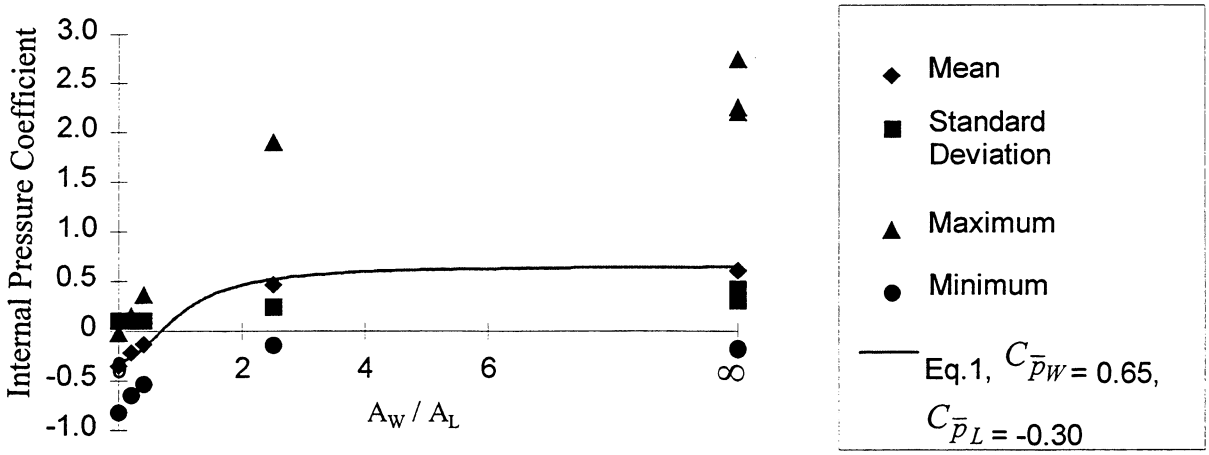

Figure 8. Mean, Standard Deviation, Maximum and Minimum Internal Pressure Coefficients vs. A_W/A_L Ratio for WERFL Test Building (Background Leakage Neglected).

4.2.1 Building Containing a Dominant Opening

A part of the measured windward wall pressure, roof windward edge pressure and internal pressure on the building with a 2% windward wall opening is shown in Figure 9a. The resultant net pressures on the windward wall and roof windward edge are shown in Figure 9b. The pressure inside the WERFL test building with a dominant windward wall opening, follows the external pressure at the opening. Yin (1994) found that the internal pressure was well correlated, positively with the windward wall pressure and negatively with the roof windward edge pressure in the WERFL test building with a dominant windward wall opening.

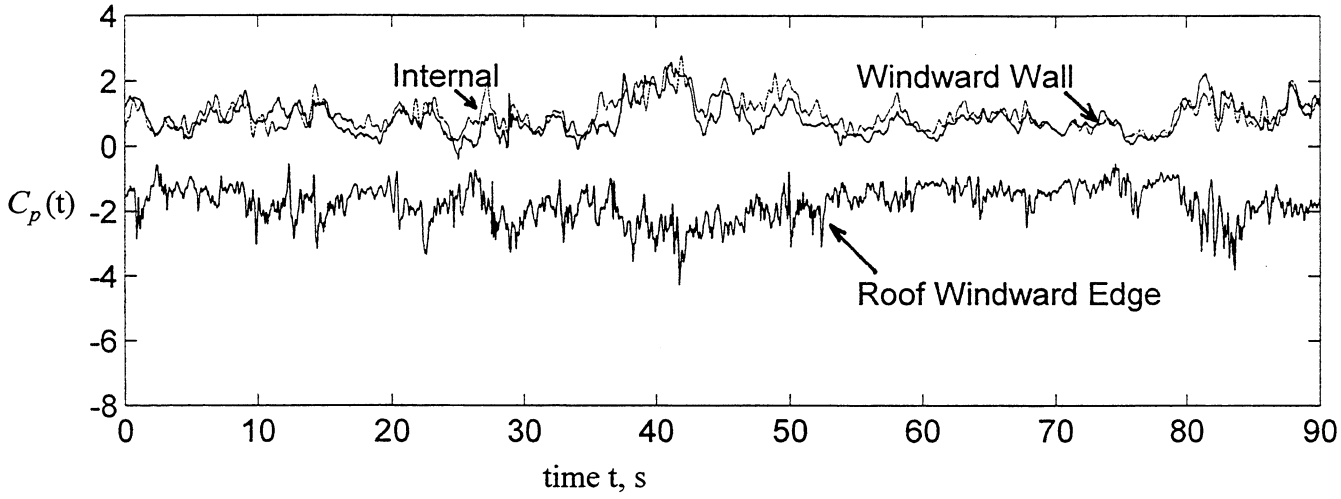

Figure 9a. Internal, Windward Wall and Windward Roof Edge Pressure Coefficient vs Time - Building with 2% Windward Wall Opening

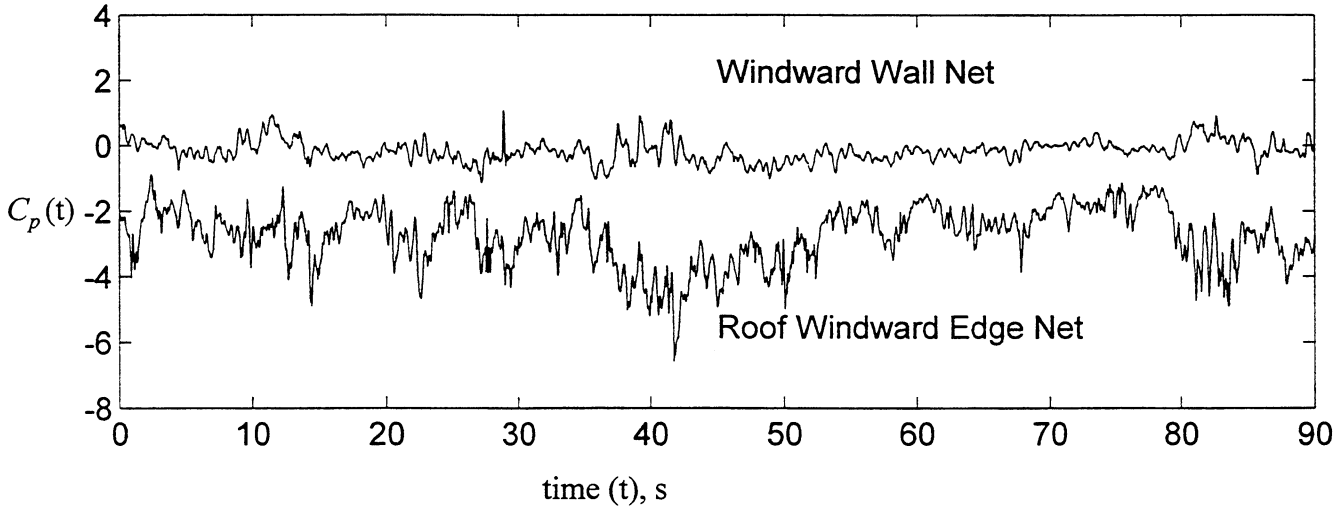

Figure 9b. Net Windward Wall and Windward Roof Edge Pressure Coefficient vs Time - Building with 2% Windward Wall Opening

The mean, standard deviation, maximum and minimum pressure coefficients, the pressure peak factors, g_p and the pressure gust factors, G_p on the windward wall, leeward wall, side wall, roof, roof windward edge and interior of the building with a 2% windward wall opening, and the pressure coefficients from AS1170.2 (K_L = 1.5 is applied to the roof windward edge for pressure acting on an area ~ 0.5 m^2 , 1.5 m from the edge) are given in Table 3a.

The transmission of external pressure at the opening into the building results in the internal pressure gust factor, and pressure peak factor being of similar magnitude to the windward wall pressure gust factor and pressure peak factor respectively.

Table 3a. External and Internal Pressure Mean, Standard Deviation, Maximum and Minimum Coefficients - Building with a 2% Windward Wall Opening

Tap Location	Pressure Coefficients					g_p	G_p
	AS1170	$C_{\bar{p}}$	C_{σ_p}	$C_{\hat{p}}$	$C_{\check{p}}$		
Windward Wall Center	0.7	0.62	0.42	2.76	-0.43	5.10	4.45
Leeward Wall Center	-0.4	-0.43	0.13	-0.09	-0.95	4.00	2.21
Side Wall Center	-0.5	-0.40	0.25	0.44	-1.99	6.36	4.98
Roof Center	-0.5	-0.37	0.17	0.39	-1.64	7.47	4.43
Roof Windward Edge	-1.35	-1.28	0.52	0.12	-4.68	6.54	3.65
Internal	0.7	0.61	0.42	2.74	-0.38	5.07	4.49

The peak net (external - internal) pressure coefficients are compared with the (peak external - peak internal) values shown within parenthesis and the equivalent net values derived from AS1170.2 in Table 3b. A velocity gust factor G_U = 1.75 for 4.0 m in terrain category 2 (AS1170.2) is used in Equation 9 to calculate the equivalent AS1170.2 net C_{pk} value.

Table 3b. Mean, Standard Deviation, Maximum and Minimum Net Pressure Coefficients Building with a 2% Windward Wall Opening

Tap Location	Net Pressure Coefficients					
	AS1170.2		Measured			
	$C_{\bar{p}}$	C_{pk}	$C_{\bar{p}}$	C_{σ_p}	$C_{\hat{p}}$	$C_{\check{p}}$
Windward Wall Center	0.0	0.0	0.01	0.25	1.46 (3.14)	-1.47 (-3.17)
Leeward Wall Center	-1.1	-3.37	-1.04	0.48	-0.03 (0.29)	-3.42 (-3.69)
Side Wall Center	-1.2	-3.68	-1.01	0.58	0.11 (0.82)	-3.96 (-4.73)
Roof Center	-1.2	-3.68	-0.98	0.47	0.02 (0.77)	-3.98 (-4.38)
Roof Windward Edge	-2.05	-6.27	-1.89	0.86	-0.22 (0.50)	-6.91 (-7.42)

The measured peak net pressures were smaller in magnitude compared to the (peak external - peak internal) pressures in most regions, on the building with a 2% single windward wall opening. The large external suction pressures at the roof windward edge which is the region most susceptible to local cladding failure, were well correlated with the large positive internal pressure leading to large net pressures. The peak suction net pressure coefficient of -6.91 at the roof windward edge is 93% of the (peak external - peak internal) pressure coefficient of -7.42. The peak net pressure coefficients in most regions (including at the roof windward edge), derived from AS1170.2 were

generally unconservative, acknowledging that the measured pressures were 1/8 sec peaks acting over area of ~ 0.5m^2. Cochran and Cermak (1992) showed that peak suction pressures measured on the full scale Texas Tech building gave significantly larger values compared with wind tunnel model values. Hence codes and standards based on wind tunnel studies are liable to underestimate peak pressures near edge discontinuities. Ginger and Letchford (1995) also found that the local pressure factors K_L derived from a wind tunnel study on a low-rise model were larger than those given in AS1170.2.

The internal pressures in the WERFL test building were simulated using a finite difference numerical technique by applying the external pressures measured on the wall containing the dominant opening (p_E) to the right hand side of Equation 4. The mean velocity at roof height $\bar{}$, the density of air ρ and the barometric pressure p_0 measured in the field were applied as input data. An adiabatic process (ie. coefficient n = 1.4) was used to calculate a_s and the effective internal volume $_{Ie}$ was 470 × 2.5 = 1175 m^3. The internal pressures were simulated for C_I = 0.89 and loss coefficient C_L values of between 2.0 and 100.

The measured and simulated (C_L = 2.68 and C_L = 8.2) internal pressure-time histories obtained for a part of a single 15 min run in the WERFL building with a 2% windward wall opening (ie. A_W = 0.8 m^2, $A_W^{3/2}/V_{Ie}$ = 0.0006), are shown in Figure 10. The windward wall pressure spectrum and the measured and simulated (C_L = 2.68 and C_L = 8.2) internal pressure spectra, $fS_p(f)/\left(\frac{1}{2}\rho\bar{U}^2\right)^2$ for the building with 2% windward wall opening (ie. A_W = 0.8 m^2) are shown in Figure 11. Measured and simulated pressure spectra for 1% and 5% windward wall openings and 5% leeward wall opening were given in Ginger et al (1995). The variation of internal pressures with time in Figure 10 and the spectra in Figure 11, show that the numerical scheme using C_L = 8.2, simulates the measured internal pressures better than that using the "accepted" value of C_L = 2.68.

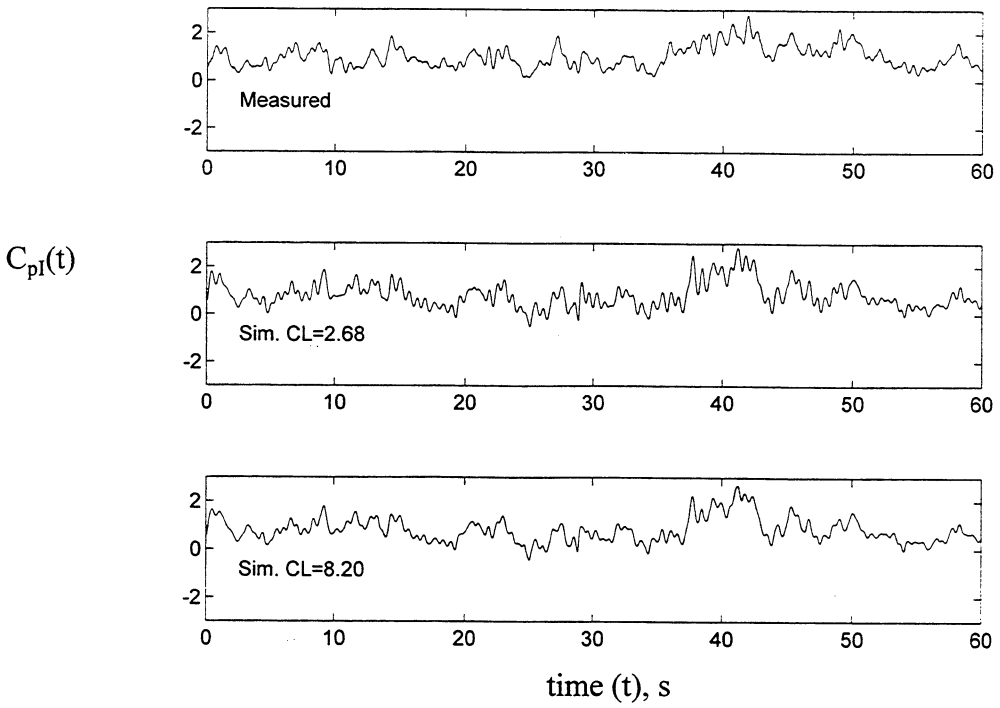

Figure 10. Measured and Simulated Internal Pressure vs Time - Building with 2% Windward Wall Opening

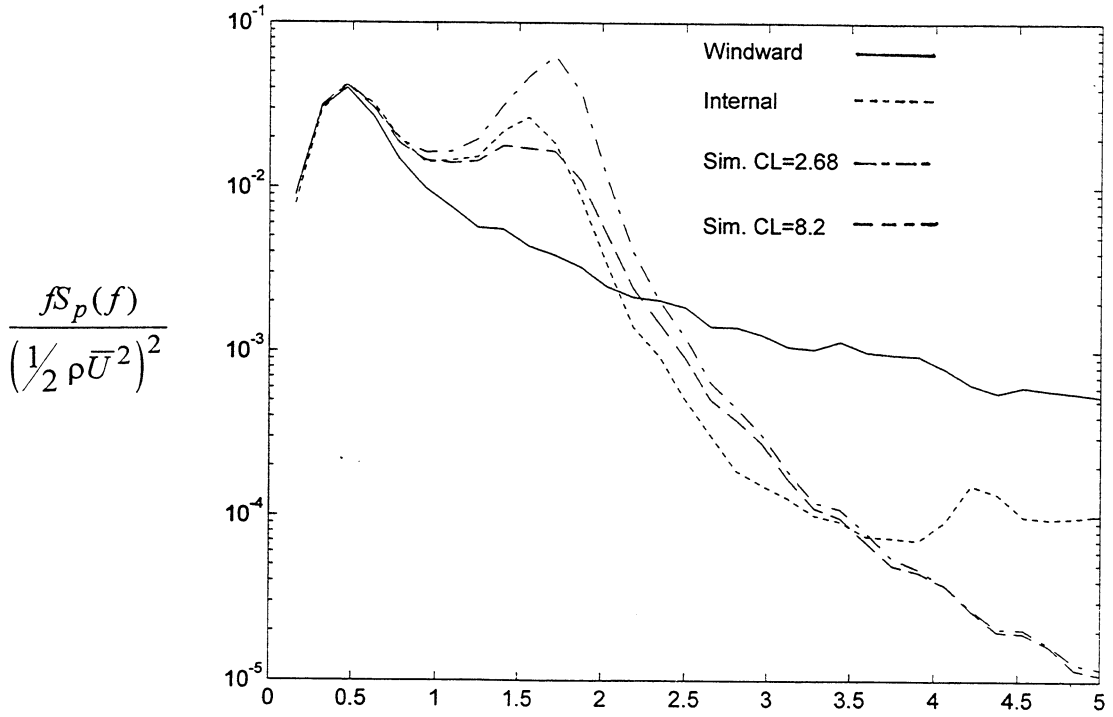

Figure 11. Non-dimensional Windward Wall, and Measured and Simulated (C_L = 2.68 and C_L = 8.2) Internal Pressure Spectra - Building with 2% Windward Wall Opening

In Figure 11, the measured internal pressure spectrum, for the building with 2% single windward wall opening, shows an increase of internal pressure energy close to the Helmholtz frequency, f_0 of 1.58 Hz compared with the windward wall pressure fluctuations. Similar increases in internal pressure energy were also found by Ginger et al (1995) for the 1% opening at 1.34 Hz and the 5% opening at 2.00 Hz. As the opening area increases from 1% to 5% this resonant peak in the internal pressure spectrum also increases, and there is a greater tendency for resonance to occur.

Application of measurements from the building with a 2% windward wall opening case to Equation 5, gives $C_{\sigma pI}/C_{\sigma pE}$ = 1.15. Therefore a measured value of $C_{\sigma pE}$ = 0.42, gives $C_{\sigma pI}$ = 0.48 which compares with the measured value of $C_{\sigma pI}$ = 0.42 as shown in Table 3a.

The pressure spectra $fS_p(f)/\left(\frac{1}{2}\rho\overline{U}^2\right)^2$ for windward wall, roof windward edge and interior of the building with a 2% windward wall opening are presented in Figure 12. The net pressure spectra

on the windward wall, and roof windward edge of the building with a 2% windward wall opening are shown in Figure 13. Figure 13 shows that the net pressure energy increases near the Helmholtz frequency of 1.58 Hz, compared with the windward wall pressure fluctuations shown in Figure 12. The increase in internal pressure energy near the Helmholtz frequency influences the net pressure fluctuations as shown by the increase in energy near the Helmholtz frequency in the net windward wall and roof windward edge pressure spectra. This increase in energy can increase loads on cladding components and fixtures and accelerate fatigue failure at cladding connections.

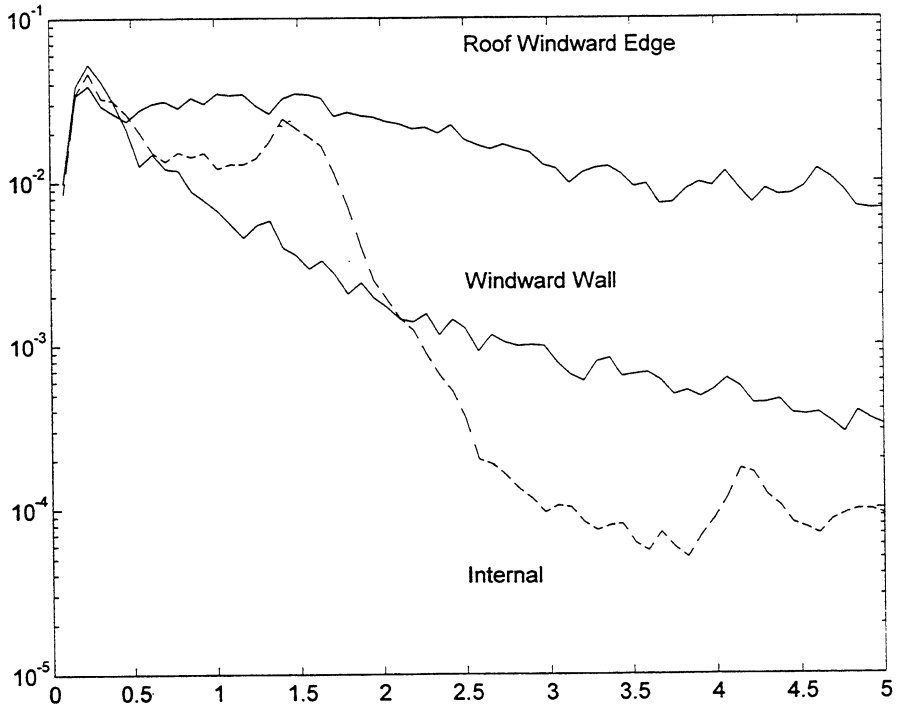

Figure 12. Non-dimensional Windward wall, Roof Windward Edge and Internal Pressure Spectra - Building with 2% Windward Wall Opening

A loss coefficient C_L of 2.68 equivalent to an orifice discharge coefficient k of 0.61, is applicable under steady flow conditions. However, this study shows that under highly fluctuating and reversed flow conditions, as in the case of a dominant opening, the value of C_L is in the range of 8.0 to 45, for an assumed C_I of 0.89. Holmes (1979) also obtained an orifice discharge coefficient k in the range of 0.15 to 0.35 under highly fluctuating and reversed flow conditions for a dominant windward opening and found similar resonance effects in his model study.

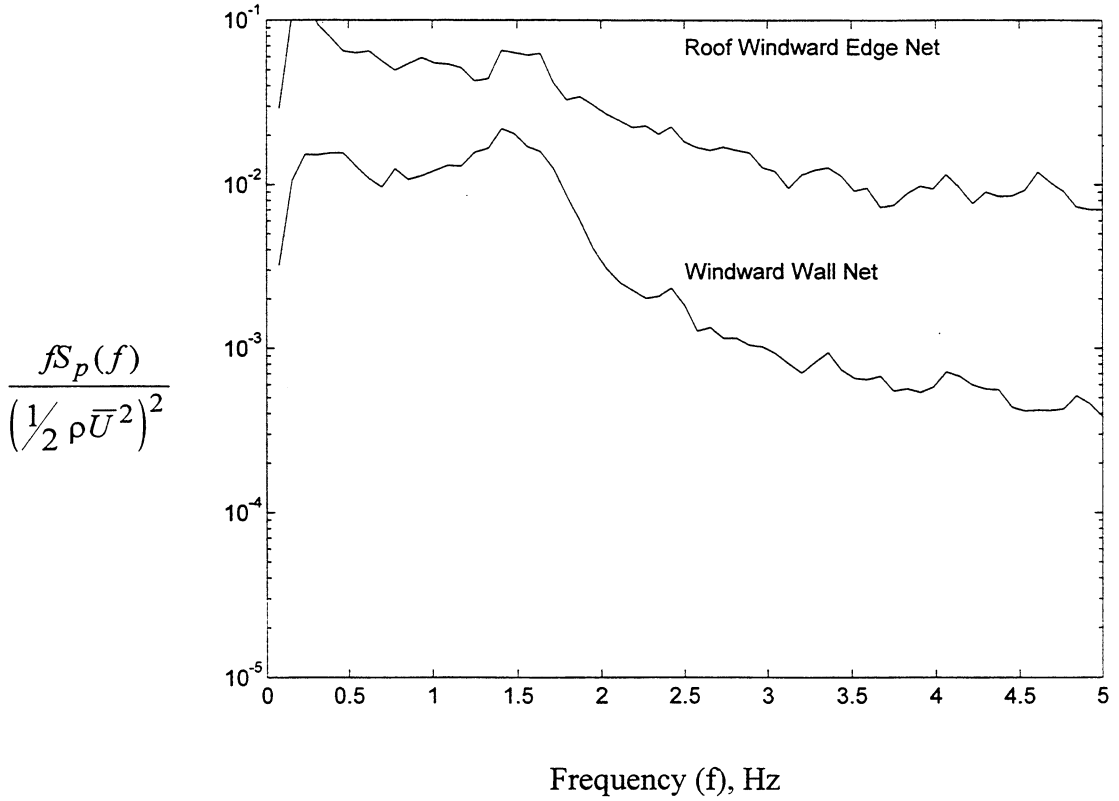

Figure 13. Non-dimensional Windward wall, Roof Windward Edge Net Pressure Spectra - Building with 2% Windward Wall Opening

5. SAMPLE CALCULATIONS

The theories described in this report are used to determine the internal pressures for the cases of a nominally sealed building and a building with a dominant windward opening. The results are compared with values given in AS1170.2 in this section.

- Example #1 Nominally Sealed Domestic Building

Rectangular Plan 20m × 10m × 3m high Building
Nominally Sealed (Porosity $\varepsilon = 5 \times 10^{-4}$)
Ceiling provides a non-porous barrier between inside and roof space
Stiff Building (ie. $K_A/K_B = 0$) $V_{Ie} = V_I(1+0) = 20 \times 10 \times 3 = 600$ m^2
Building is located in Suburbs (Terrain Category 3 AS1170.2)
Turbulence Intensity at roof height = 0.30
Integral Length Scale L_U = 120m
Design Mean Wind Speed at Roof Height $\overline{U}$ = 20 m/s

Assume wind flow is normal to the 20 × 3 m face and use data from AS1170.2
Average mean pressure coefficient on the Windward wall is +0.7

Average mean pressure coefficients on the side walls and leeward wall -0.455 and -0.5 respectively
"Windward" opening area = 60 × 0.0005 = 0.03 m^2 *"Leeward"* opening area = 0.06 m^2.
Windward and leeward pressure coefficients for use in Eqns 2 & 14 are +0.7 and -0.478 respectively

The mean internal pressure coefficient derived from Equation 2 is = -0.242.

The value of f_C computed from Equation 14 is 0.145 Hz, and $f_C L_U / \overline{U} = 0.868$

From Figure 2 from Vickery (1986) $\upsilon L_U / \overline{U} = 0.46$ and $\upsilon = 0.077$ and $\sigma_U(f_C) / \sigma_U = 0.9$.
For T = 1hr = 3600s, $\upsilon T = 276$, and From Equation 12, $g_u = 3.53$,
$\sigma_U(f_C) / \overline{U} = 0.9 \times 0.30 = 0.27$ and From Equation 10, $G_{pI} = 2.91$
The range of C_{pI} due to wind speeds averaged over a period of 1/fc (ie 7 sec) will be -0.70 to 0.22
The equivalent peak internal pressures given by AS1170.2 are -0.92, and 0 respectively.

- Example #2 Industrial Type Building with a Dominant Windward Wall Opening

Square Plan 20m × 20m × 10m High Building
6m × 8m Windward Opening Centered z = 3m above Ground (Background Porosity $\varepsilon = 5 \times 10^{-4}$)
Flexible Building (ie. $K_A/K_B = 1.2$)
Effective Volume $V_{Ie} = V_I (1+ 1.2) = 4000 \times 2.2 = 8800\ m^3$
Building is located in Open Fetch (Terrain Category 2 AS1170)
Turbulence Intensity at roof height = 0.183
Integral Length Scale $L_U = 120$m
Design Mean Wind Speed at Roof Height $\overline{U} = 36$ m/s

According to Vickery (1994) $S_O = fS(f)/\sigma_U^2 = 0.045\left(f_0 z/\overline{U}(z)\right)^{-2/3}$

For z = 3.0m $\overline{U} = 29$ m/s

$S_O = 0.204\ f_O^{-2/3}$

For $a_s = 340$ m/s and $C_I = 0.89$ from $f_0 = \frac{1}{2\pi}\left(\frac{340^2\sqrt{48}}{(0.89)(8800)}\right)^{1/2} = 1.61$ Hz $S_O = 0.149$,

Equation 7 gives, $\beta = \frac{1}{2}\left(\frac{C_L}{C_I}\right)^{1/2} \frac{\overline{U}}{a_s}\sqrt{V_{Ie}}A^{-3/4} = \frac{1}{2}\left(\frac{2.68}{0.89}\right)^{1/2} \frac{29}{340}\sqrt{8800}(48)^{-3/4} = 0.381$

For $C_{\sigma pE} = 0.35$, From Equation 5, $C_{\sigma pI}/C_{\sigma pE} = 1.67$

The $C_{\sigma pI}$ would then be 0.59. For a mean internal pressure coefficient of 0.65, applying a pressure peak factor of $g_p = 5.0$ this would give a peak internal pressure coefficient of 3.58 which corresponds to an internal pressure gust factor of 5.51 or an internal pressure coefficient of 1.23 based on 3 second gust speed at roof height of 3m used in AS1170.

6. CONCLUSIONS AND RECOMMENDATIONS

Recent studies have shown the importance of internal pressure effects in the design of roof and wall cladding. Partly due to these studies, wind load standards have been updated with more reliable values. Typically wind load standards provide a range of internal pressure coefficients depending on the openings in the building envelope (ie. nominally sealed, windward/leeward openings). Equation 2 is used as the basis for deriving these pressure coefficients in AS1170.2. The results of this study given in Section 4, show that the updated values prescribed in AS1170.2 generally give satisfactory estimates of internal pressure and may be used with confidence in low-rise building design. Some further refinements will be possible with more detailed research into areas such as net pressures, Helmholtz resonance and area averaged pressures.

A combination of theoretical analysis, numerical simulation and full scale measurements on the WERFL low-rise test building at Texas Tech, when nominally sealed and with large openings has been used to investigate wind generated internal pressures. Full scale measurements of external and internal pressures obtained on the WERFL test building were used to study the characteristics of the net pressures acting on various parts of the building. The measured net pressures were compared with values derived from AS1170.2 used for determining design loads on cladding elements and fixings. The following conclusions are obtained from this study;

The mean and fluctuating internal pressure coefficients in a nominally sealed building were smaller in magnitude than the pressure on the external surfaces. Mean and fluctuating internal pressure coefficients increase with increasing windward/leeward open area ratio. The measured mean internal pressure coefficients agree with the values obtained from the theoretical analysis of "steady flow" through an orifice.

The internal pressure fluctuations were influenced by the interaction of internal air volume with the building. The effect of building flexibility in slowing the internal pressure response was accounted for by increasing the nominal internal volume (V_I) by a factor of the ratio of bulk modulus of air (K_A) to the bulk modulus of the building (K_B). The experimental results were in good agreement with the theoretical analysis carried out using an effective interior volume of $_{Ie}$ equal to $_{I} \times \left(1+\left(K_A/K_B\right)\right)$.

Internal pressure fluctuations especially those above the characteristic frequency f_C were significantly attenuated in the nominally sealed WERFL test building. This resulted in a smaller internal pressure gust factor compared with the windward wall external pressure gust factor as shown by Vickery (1986). Wind load standards (ie. AS1170.2) provide conservative peak internal pressures for buildings with porosities comparable to the WERFL test building. The peak net pressures derived from AS1170.2 on most parts of nominally sealed building were conservative compared with the measured values. The peak net pressure coefficients on the nominally sealed WERFL test building were 76% to 90% in magnitude compared with the (peak external -peak internal) pressures.

The internal pressures closely followed the windward wall pressure fluctuations in the WERFL test building containing a dominant windward wall opening. A windward wall opening resulted in reduced net positive loads on the windward wall and increased net negative loads on the roof, side walls and leeward wall compared to that of the nominally sealed building. The peak net pressures derived from AS1170.2 on some parts such as the roof windward edge region of the building with a

dominant windward opening were generally unconservative compared with the measured values. The net peak suction pressure in this region was 93% of the (peak external - peak internal) value which indicates that the large positive internal pressures and the large suction roof windward edge pressures were well correlated.

The measured internal pressure spectra show an increase of pressure energy close to the Helmholtz frequency, f_0, compared with the pressure fluctuations at the opening for a building with a dominant opening. An increase in the area of the opening reduces the damping and increases the tendency for resonance. The time history and spectra of simulated internal pressure with a loss coefficient, C_L between 8.2 and 45 for $C_I = 0.89$, is in good agreement with the measured internal pressures. Holmes (1979) arrived at similar conclusions from his wind tunnel model study of a building with a single dominant windward opening.

Theories used in this study and typical pressure data were applied to the design of a nominally sealed building and a building with a dominant windward opening. The results showed that AS1170.2 will generally produce conservative net pressures even in the windward roof edge region, except possibly for small areas corresponding to roof connections near the edges. Cochran and Cermak (1992) showed that extreme external peak suction pressures of greater magnitude were measured over local areas near edge discontinuities, especially for oblique wind directions in the full-scale studies at Texas Tech compared with model tests. These large external suction pressures combined with large positive internal pressures in the case of a building with a dominant windward opening can generate net pressures larger than that given by AS1170.2. Ginger and Letchford (1995) also showed that local pressure factors K_L given in AS110.2 in some regions were smaller than the values obtained from a wind tunnel model study. More detailed systematic area averaged full-scale pressure studies are required to confirm this and generate quantitative results. Recommendations may then be made to increase the value of the local pressure factors given in AS1170.2.

7. ACKNOWLEDGMENTS

The author wishes to thank the Director Dr. Kishor Mehta, and Staff at the Wind Engineering Research Center at Texas Tech University for providing the opportunity to collect and analyze most of the data used in this study.

8. REFERENCES

1. AS-1170.2 (1989), Australian Standard SAA loading code Part 2, Wind Loads.
2. ASCE7-95, ASCE Standard Minimum Design Loads for Buildings and Other Structures
3. Cochran, L. S. and Cermak, J. E. (1992), Full and model scale cladding pressures on the Texas Tech University experimental building, Jour. of Wind Engg and Industrial Aerodyn, Vol. 43., 1589-1600.
4. Ginger, J. D., Yeatts, B. B. and Mehta, K. C. (1995), "Internal pressures in a low-rise full scale building", Proc. 9th International Conference on Wind Engineering, New Delhi, India, Jan 1995.
5. Ginger, J. D., and Letchford, C. W. (1995), Pressure factors for edge regions on low-rise building roofs", Jour. of Wind Engg and Industrial Aerodyn, Vol. 54/55., 337-344.

6. Ginger, J. D., and Letchford, C. W. (1997), "Net Pressure on Low-rise Full Scale Buildings", Proc. IVAPSOWE Gold Coast Australia July 1997.
7. Ginger, J. D., Mehta K. C. and Yeatts B. B(1997), "Internal Pressures in a Low-Rise Full Scale Building", (Accepted Jour. of Wind Engineering and Industrial Aerodynamics.
8. Greenway, M. E. (1979), An analytical approach to wind velocity gust factors, Jour. of Industrial Aerodyn, Vol. 5., 61-91.
9. Harris, R. I. (1990), The Propagation of internal pressures in buildings, Jour. of Wind Engg and Industrial Aerodyn, Vol. 34., 169-184.
10. Holmes, J. D. (1979), Mean and Fluctuating Internal Pressures Induced by wind, Proc. 5th Int. Conf. on Wind Engg., Colorado USA, Vol. 1, 435-450.
11. Holmes, J. D. (1981), Wind loads on low-rise buildings, Dept. of Civil and Systems Engineering, James Cook University, Research Report.
12. Kawai, H. (1983), Pressure fluctuations on square prisms - Applicability of strip and quasi-steady theory, Jour. of Wind Engg and Industrial Aerodyn, Vol. 13., 197-208.
13. Kramer, C., Gerhardt, H. J. and Scherer, S. (1979), "Wind Pressure on Block Type Buildings", Jour. of Industrial Aerodyn, Vol. 4, 229-242.
14. Levitan, M. L. and Mehta, K. C. (1992a, 1992b), Texas Tech Field Experiments for Wind Loads Part I: Building and Pressure Measurement System, Part II: Meteorological Instrumentation and Terrain Parameters, Jour. of Wind Engg and Industrial Aerodyn, Vol. 43., 1565-1588.
15. Liu, H. (1978), "Building Code Requirements on Internal Pressure", 3rd US Conf. of Wind Engineering Research, Florida, USA, VI-7.
16. Liu, H. and Saathoff, P. J. (1981), "Building Internal Pressure: Sudden Change", Jour. of The Engineering Mechanics Division, Vol. 107, No. EM2, 309-321.
17. Liu, H. and Rhee, K. H. (1986), "Helmholtz Oscillation in Building Models", Jour. of Wind Engineering and Industrial Aerodyn, Vol. 24, 95-115.
18. Stathopoulos, T., Surry, D. and Davenport, A. G. (1979), "Internal Pressure Characteristics of Low-rise Buildings due to Wind Action", Proc. 5th Int. Conf. on Wind Engg., Colorado USA, Vol. 1, 451-463.
19. Thomas, G., Cochran, L., Cermak J. E. and Mehta K. C. (1993), " Comparison of Field and Wind Tunnel Measured Spectra", Proc. 7th US National Conference on Wind Engineering, UCLA, Los Angeles USA.
20. Vickery, B. J. (1986), Gust factors for internal pressures in low rise buildings, Jour. of Wind Engg and Industrial Aerodyn, Vol. 23., 259-271.
21. Vickery, B. J. (1991), "Comments on "The Propagation of Internal Pressures in Buildings" by R I Harris", Jour. of Wind Engineering and Industrial Aerodyn, Vol. 37, 209-212.
22. Vickery, B. J. and Georgiou P. N. (1991), "A Simplified Approach to the Determination of the Influence of Internal Pressures on the Dynamics of Large Span Roofs", Jour. of Wind Engineering and Industrial Aerodyn, Vol. 38, 357-369.
23. Vickery, B. J. and Bloxham, C. (1992), "Internal Pressure Dynamics with a Dominant Opening", Jour. of Wind Engineering and Industrial Aerodyn, Vol. 41, 193-204.
24. Vickery, B. J. (1994), Internal Pressures and Interactions with the Building Envelope, Jour. of Wind Engg and Industrial Aerodyn, Vol. 53., 125-144.
25. Yeatts, B. B. and Mehta, K. C. (1993), Field experiments for building aerodynamics, Jour. of Wind Engg and Industrial Aerodyn, Vol. 50., 213-224.
26. Yin, J. (1994), Reliability of low-rise buildings under wind loads, PhD Research Proposal, Texas Tech University, Lubbock Texas, USA.